Interferences in laser assisted photoionization of diatomic molecules

2014 J. Phys.: Conf. Ser. 488 012021

(http://iopscience.iop.org/1742-6596/488/1/012021)

XXVIII International Conference on Photonic, Electronic and Atomic Collisions (ICPEAC 2013) IOP Publishing
Journal of Physics: Conference Series **488** (2014) 012021 doi:10.1088/1742-6596/488/1/012021

Interferences in laser assisted photoionization of diatomic molecules

D I R Boll[1], O A Fojón[1,2]

[1]Instituto de Física Rosario, CONICET-UNR, Pellegrini 250, 2000 Rosario, Argentina
[2]Escuela de Ciencias Exactas y Naturales, Universidad Nacional de Rosario, Argentina.

E-mail: fojon@ifir-conicet.gov.ar

Abstract. We analyze interference effects in photoionization of H_2^+ molecular targets in laser assisted photoionization. By means of a simple model, we obtain observables for the reaction and we compare them with previous results obtained with more elaborated ones. Interestingly, previous interference effects predicted for monochromatic pulses persist in the presence of a laser NIR bath leading to a characteristic photoelectron spectrum.

1. Introduction

In the last decade, the development of extreme ultraviolet (XUV) pulses with durations of a few hundreds of attoseconds has opened the way to a new and fascinating branch of physics, intimately related to atomic and molecular physics [1]. After the achievements obtained with their predecesors, femtosecond laser pulses during the nineties, these attosecond pulses (ATP) allow now the study of photoionization dynamics with unprecedent time resolution close to the electronic time scale. Moreover, in the so called pump-probe experiments ([1] and references therein) where the reaction is assisted with a near infrared (NIR) laser, it is possible to extract information about ATP [2] as well as monitoring and/or steering electron dynamics in atoms and molecules [3, 4] and mapping molecular wave-packets [5]. In this perspective, both single ATP (SATP) and attosecond pulse trains (ATPT) turn out to be promising tools to control the electronic charge density in atomic and molecular systems [4, 6, 7]. Several works are devoted to the characterization of SATP and ATPT [8, 9] and the widespread experimental procedure is the conversion of them into electron wave packets by means of photoionization of atoms assisted by a NIR laser field. The same scheme may be used to control electronic emission from atomic and molecular systems.

On the experimental front, APT are usually created by high harmonic generation (HHG) procedures by which basically a comb of almost equally strong harmonics could be obtained by focusing an intense ultrashort infrared laser pulse into a noble gas atom [10]. ATPT are produced naturally from the HHG process when the driving laser field is many periods long.

On the theoretical side, the numerical resolution of the time dependent Schrödinger equation for reactions such as the photoionizatoin of molecular targets assisted by a NIR laser represent a computational challenge [11, 12, 13]. In this context, the use of a simplified model leading to reasonable results could be very helpful to understand the underlying physical processes. Among them, we could mention the Strong Field Approximation (SFA) in which the electron is suposed to evolve without interact with the coulomb field created by the target [14]. An improvement on

this approximation is given by the Separable Coulomb-Volkov (SCV) model to treat atomic or molecular targets [15, 16, 17]. In the SCV approach, there are three time steps in the electronic evolution. In the first one, the ionized electron evolves as if it were subject exclusively to the coulomb field of the target whereas in the third and last interval of time, photoelectrons are described by the Volkov continuum irrespective of the relative importance of coulomb and laser fields [16]. In the intermediate step, both the coulomb and NIR laser fields are acting on the ejected electron and are of comparable importance. It is worthy to mention that the SCV for the case of simple molecular targets described by linear combination of atomic orbitals (LCAO) leads to analytical expressions simplifiying the computation of the observables for the reaction.

In this work, we show that the SCV model gives a qualitative agreement with ab initio calculations of photoionization cross sections [18, 19, 20] of H_2^+ molecules and then we analyze the case where the reaction is assisted by a NIR laser. The initial molecular wavefunctions are described here as a linear combination of Slater type orbitals (STOs) variationally optimized whereas the final wavefunctions are SCV type wavefunctions [16]. Employing these initial and final wavefunctions, analytical expressions for the observables of interest, namely, photoionization spectrum, multiple differential cross sections, photoelectron angular distributions (PADS), etc, are obtained.

Atomic units are used otherwise explicitely stated.

2. Theory

Let us consider the photoionization of a diatomic molecule through SATP assisted by a monochromatic NIR laser. To fix ideas, we consider the case of the H_2^+ targets as its theoretical description is simpler than other multielectronic molecules. In the following, we summarize the basics ingredients of the SCV model [16].

The coordinate system used is one where $\mathbf{R}$ is the internuclear vector pointing from nuclei 1 to 2 and $\mathbf{r}_i$ denotes the electron position vector with respect to the i-th nuclei. The electron coordinate with respect to the molecular center of mass will be given by $\mathbf{r} = (\mathbf{r}_1 + \mathbf{r}_2)/2$.

The matrix transition amplitude corresponding to the photoionization reaction of a diatomic molecule by an SATP in the extreme ultraviolet regime (XUV) in the presence of a NIR laser bath in the velocity gauge is given by,

$$M_{scv}(\mathbf{p}) = -i \int_{-\infty}^{\infty} dt \langle \Psi_f(\mathbf{r}, t) | \hat{\mathbf{p}} \cdot \mathbf{A}(t) | \Psi_i(\mathbf{r}, t) \rangle, \tag{1}$$

where $\hat{\mathbf{p}}$ is the momentum operator, and $\Psi_i(\mathbf{r}, t)$ and $\Psi_f(\mathbf{r}, t)$ are the initial and final wavefunctions corresponding to the initial and final channels of the reaction, respectively.

The vector potential $\mathbf{A}(t)$ representing the XUV pulse is given by,

$$\mathbf{A}(t) = \mathbf{\Pi}(\phi) A_0 e^{-i\Omega t} \exp\left[-\frac{(t - t_0)^2}{2\tau^2} \right], \tag{2}$$

$$= \mathbf{\Pi}(\phi) A_0 \tau \sqrt{\frac{1}{2\pi}} \int_{-\infty}^{\infty} R(\Omega) e^{-i(\omega + \Omega)t} \, d\omega, \tag{3}$$

where Ω is the central frequency of the attosecond pulse. $\mathbf{\Pi}(\phi)$, A_0 y t_0 are the polarization vector, the amplitude and delay of the pulse, respectively. The duration of the attopulse denoted by τ is related to its full width half maximum (FWHM) through $\tau_{FWHM} = 2\sqrt{\ln 2}\ \tau$. The interference factor represented by $R(\Omega)$ in Eq. 3 is given by,

$$R(\omega) = \exp[i\omega t_0 - \omega^2 \tau^2 / 2]. \tag{4}$$

For low and intermediate NIR laser intensities ($I < 10^{14} \mathrm{W/cm}^2$) one can reasonably approximate the bound states by *laser-free* wavefunctions, *i.e.*,

$$\Psi_i(\mathbf{r},t) = \psi_i^0(\mathbf{r})\exp(iI_p t), \tag{5}$$

where I_p is the ionization potential of the molecule. We describe the continuum states of the electron by the Coulomb-Volkov *ansatz* [15] in which the interaction of the ejected electron with both the residual ionic target and the laser bath is taken into account,

$$\Psi_f(\mathbf{r},t) = \psi_f^0(\mathbf{r})\exp\left\{-\frac{i}{2}\int^t [\mathbf{p}+\mathbf{A}_L(t)]^2\, dt\right\}, \tag{6}$$

with $\mathbf{p}$ the asymptotic value of the photoelectron momentum and $\mathbf{A}_L(t)$ the potential vector describing the NIR laser field. The wavefunctions $\psi_i^0(\mathbf{r})$ and $\psi_f^0(\mathbf{r})$ describe the bound and continuum states of the unperturbed molecular Hamiltonian, *i.e.*, in absence of the XUV pulse and NIR laser field. The phase multiplying the $\psi_f^0(\mathbf{r})$ wavefunction in Eq. 6 is the well-known Volkov phase describing an electron of momentum $\mathbf{p}$ in the presence of an electromagnetic field given by its potential vector ($\mathbf{A}_L$ in our case). As exact wavefunctions for the reaction of interest are in general available only in numerical form, we consider in this work approximate analytical wavefunctions that simplify the computation of the corresponding matrix transition element. For the bound states, we employ two-center developements in terms of Slater type functions located on each molecular center whereas for the continuum states we used asymptotic coulombic wavefunctions satisfying the correct asymptotic coulombic conditions,

$$\psi_i^0(\mathbf{r}) \quad = \textstyle\sum_i c_i^{(1)}\phi_i(\mathbf{r}_1) + \sum_j c_j^{(2)}\phi_j(\mathbf{r}_2) \tag{7}$$

$$\psi_f^0(\mathbf{r}) \quad = (2\pi)^{-3/2} e^{i\mathbf{p}\cdot\mathbf{r}} N_p^2\, G(\mathbf{r}_1)G(\mathbf{r}_2) \tag{8}$$

where $\phi_i(\mathbf{r})$ are STO's, $N_p = \Gamma(1+i\nu)\ \exp(\pi\nu/2)$ and $G(\mathbf{r}_i) = {}_1F_1(-i\nu;1;-1(pr_i+\mathbf{p}\cdot\mathbf{r}_i))$ is the confluent hypergeometric function. The Sommerfeld parameter reads $\nu = Z/p$ with Z being the residual effective charge of the i-esime atom.

Vector potential corresponding to the NIR laser field could be written as

$$\mathbf{A}_L(t) = -\frac{\mathbf{E}_1}{\omega_1}\sin(\omega_1 t) + \frac{\mathbf{E}_2}{\omega_2}\sin(\omega_2 t + \phi_L) \tag{9}$$

where $\omega_{1,2}$ is the laser field frequency corresponding to the mutually perpendicular electric field components $\mathbf{E}_{1,2}$, respectively and ϕ_L is an arbitrary phase. The respective electric field is given thus by

$$\mathbf{E}_L(t) = -\frac{d\mathbf{A}_L}{dt} \approx \mathbf{E}_1\cos(\omega_1 t) + \mathbf{E}_2\cos(\omega_2 t + \phi_L). \tag{10}$$

Replacing Eqs. 3 and 9 into Eq. 1, and making use of the Jacobi-Anger developement [15, 16] to expand the time-dependent terms in the Volkov phase, the matrix transition amplitude given by Eq. 1 may be rewritten as,

$$\begin{aligned} M_{scv}(\mathbf{p}) = A_0\tau\sqrt{2\pi}M_{ph}(\mathbf{p}) \sum_{m_{1,2},n_{1,2}=-\infty}^{\infty} & i^{n_1+n_2}(-1)^{m_1+m_2}R(\omega)J_{m_1}(M_1)J_{m_2}(M_2) \\ & \times J_{n_1}(N_1)J_{n_2}(N_2)e^{i(2m_2+n_2)\phi_L} \end{aligned} \tag{11}$$

where we have defined,

$$M_{1,2} = E_{1,2}/(2\omega_{1,2})^3, \tag{12}$$

$$N_{1,2} = \mathbf{p}\cdot\mathbf{E_{1,2}}/\omega_{1,2}^2, \tag{13}$$

$$\omega = p^2/2 + I_p - \Omega + (2M_1 + 2m_1 + n_1)\omega_1 + (2M_2 + 2m_2 + n_2)\omega_2 \tag{14}$$

and monochromatic transition matrix element $M_{ph}(\mathbf{p})$ is given by

$$M_{ph}(\mathbf{p}) = -i\langle\psi_f^0(\mathbf{r})|\Pi(\phi)\cdot\nabla|\psi_i^0(\mathbf{r})\rangle. \tag{15}$$

To obtain $M_{ph}(\mathbf{p})$, we employ the Coulomb continuum approximation [15, 16] in which,

$$M_{ph}(\mathbf{p}) = \chi_1\, M_1 + \chi_2\, M_2, \tag{16}$$

where the molecular interference factors denoted by $\chi_{1,2}$ are given by,

$$\chi_{1,2} = N_p^* e^{\pm i\mathbf{p}\cdot\mathbf{R}/2}\, {}_1F_1(i\nu; 1; i(pR \mp \mathbf{p}\cdot\mathbf{R})), \tag{17}$$

and the $M_{1,2}$ factors correspond to atomic transition matrix amplitudes from the molecular centers $1, 2$, respectively.

Therefore, the photoelectron spectrum is given by,

$$\frac{d^3P_{scv}}{dp\; d\Omega_e} \equiv S(p, \theta_e, \phi_e) = p^2|M_{scv}(\mathbf{p})|^2. \tag{18}$$

where $d\Omega_e = \sin\theta_e\, d\theta_e\, d\phi_e$ denotes de solid angle in the direction of the asymptotic momentum of the photoelectron.

3. Results

In this section we compare the SCV results with more elaborated ones [11, 12, 13]. At first, we test our monochromatic transition amplitude by computing our PADS for H_2^+ targets with a definite spatial orientation and an XUV pulse with both polarization vector parallel and perpendicular with respect to the internuclear vector $\mathbf{R}$. We also include the case of circular polarization.

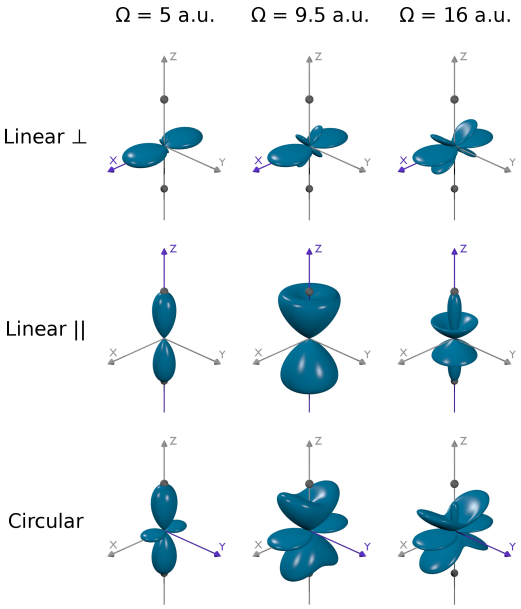

Figure 1. Monochromatic photoelectron angular distributions for H_2^+ at equilibrium internuclear separation, with XUV polarization parallel and perpendicular to the molecular internuclear separation as well as circular polarization. The nuclei are indicated by two small spheres (dark grey). For linear polarization (upper and middle panels), polarization vector is indicated by a different color axis (violet). In the case of circular polarization the violet axis indicates the incidence direction. Angular distributions (green-blue plots) for photon energies Ω =5, 9.5 and 16 a.u. correspond to an asymptotic photoelectron energy of 3.9, 8.4 and 14.9 a.u., respectively.

In Fig. 1, we present our computed PADS for three different photon frequencies Ω= 5, 9.5 and 16 a.u. for the three mentioned polarizations. To obtain the initial molecular bound state, we have used the GAMESS software package [21]. The STO-6G basis set was employed with

an additional polarization function. In the case of linear perpendicular polarization typical interferences are observed for all photon frequencies and they can be related to Young type two-slit patterns [19, 12]. As the photon energy increases, the relative magnitude of interference lobes also increases. For linear parallel polarization a different scenario appears. In general, photoelectrons are ejected mainly in the classical direction given by the polarization vector. However, for the case of $\Omega = 9.5$ a.u. ejection in this direction is partially forbiden. In turn, this can be associated to the so called confinement effect due to intereferences coming from the coherent emission from both molecular centers [19, 12]. Alternatively, this may be understood also as a Cooper minima type consequence [22]. In the case of circular polarization, our PADS exhibit a mixture of both linear parallel and perpendicular cases with an additional feature given by a *torsion* [13] of the PADS in qualitative agreement with the more elaborate results [12, 13]. Nevertheless, in our case this torsion is about 4 times smaller than in those ab-initio results. This feature is quite sensitive to the description of the molecular initial bound state and final photoelectron wavefuntion.We have checked that this *torsion* dissapears if only 1s STO's are used in the description of this initial state. Moreover, no asymmetry is observed if the final continuum wave function does not take into account the coulomb interaction with the residual target as in the SFA.

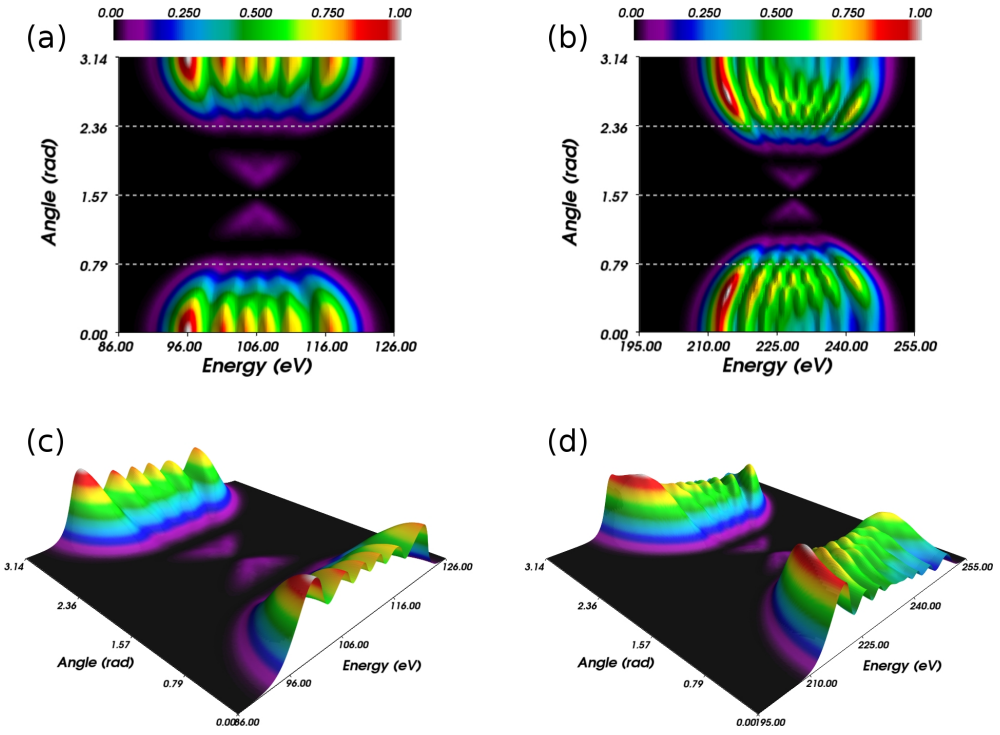

Figure 2. (a) Photoelectron spectrum in plane xz for $H2^+$ ionized by an attopulse of energy $\Omega = 5$ a.u. with a duration of 500 attoseconds linerly polarized parallel to the molecular orientation, in the presence of an equally linearly polarized NIR with a wavelength of 800 nm. NIR intensity is equal to 3.5×10^{12} W/cm^2. (b) Idem (a) but with $\Omega = 9.5$ a.u.. (c) 3D view of (a) and (d) 3D view of (b).

In Figs. 2(a) and 2(c), we present the photoelectron spectrum centered at frequency Ω= 5 a.u. for linear parallel polarization as a function of the photoelectron energy and the polar ejection angle θ_e of the photoelectrons. We observe typical sidebands located around the central frequency. As is well known, these sidebands are produced by quantum interferences occuring

during the interaction of the photoelectron with the laser NIR bath [23]. Sidebands are separated roughly by twice the NIR frequency. As the duration of XUV pulses increases reaching the period of the NIR, the separation between sidebands will be given by the NIR frequency [24, 25]. As can be seen, ejection is preferential in the alignement direction, *i.e.*, 0 and 180 degrees for the mentioned frequency. However, when we consider the frequency Ω= 9.5 a.u. (Figs. 2(b) and 2(d)), the photoelectron spectrum show a decrease for those angles. In this way, the confinement effects observed in the case of monochromatic pulses leave their trace in the photoelectron spectrum even when the NIR laser is added.

4. Conclusions

We have studied interference effects in photoionization of H_2^+ molecular targets in laser assisted photoionization. By means of a simple model, we obtain observables for the reaction in qualitative agreement with previous results obtained with more elaborated methods [12, 13]. Interestingly, previous interference effects predicted for monochromatic pulses persist in the presence of a laser NIR bath leading to a characteristic photoelectron spectrum. The present study may be extended without great effort to more complex diatomic molecules. Work in this direction is in progress.

References

[1] Krausz F and Ivanov M 2009 *Rev. Mod. Phys.* **81** 163–234
[2] Laurent G, Cao W, Li H, Wang Z, Ben-Itzhak I and Cocke C L 2012 *Phys. Rev. Lett.* **109**(8) 083001
[3] Kling M F, *et al* 2006 *Science* **312** 246–248
[4] Kelkensberg F, *et al* 2011 *Phys. Rev. Lett.* **107**(4) 043002
[5] Tong X M and Lin C D 2006 *Phys. Rev.*A **73**(4) 042716
[6] Johnsson P, Mauritsson J, Remetter T, L'Huillier A and Schafer K J 2007 *Phys. Rev. Lett.* **99**(23) 233001
[7] Singh K P, *et al* 2010 *Phys. Rev. Lett.* **104**(2) 023001
[8] Mauritsson J, Johnsson P, Gustafsson E, L'Huillier A, Schafer K J and Gaarde M B 2006 *Phys. Rev. Lett.* **97**(1) 013001
[9] He X, Dahlström J M, Rakowski R, Heyl C M, Persson A, Mauritsson J and L'Huillier A 2010 *Phys. Rev.* A **82**(3) 033410
[10] Dahlström J M, LHuillier A and Maquet A 2012 *J. Phys. B: At. Mol. Opt. Phys.* **45** 183001
[11] Hu S X, Collins L A and Schneider B I 2009 *Phys. Rev.* A **80**(2) 023426
[12] Fernández J, Yip F L, Rescigno T N, McCurdy C W and Martín F 2009 *Phys. Rev.* A **79**(4) 043409
[13] Guan X, DuToit R C and Bartschat K 2013 *Phys. Rev.* A **87**(5) 053410
[14] Reiss H 1992 *Progress in Quantum Electronics* **16** 1 – 71
[15] Yudin G L, Chelkowski S and Bandrauk A D 2006 *J. Phys. B: At. Mol. Opt. Phys.* **39** L17
[16] Yudin G L, Patchkovskii S, Corkum P B and Bandrauk A D 2007 *J. Phys. B: At. Mol. Opt. Phys.* **40** F93
[17] Yudin G L, Patchkovskii S and Bandrauk A D 2008 *J. Phys. B: At. Mol. Opt. Phys.* **41** 045602
[18] Fojón O, Palacios A, Fernández J, Rivarola R and Martín F 2006 *Phys. Lett.* A **350** 371 – 374
[19] Fernández J, Fojón O, Palacios A and Martín F 2007 *Phys. Rev. Lett.* **98** 043005
[20] Fernández J, Fojón O and Martín F 2009 *Phys. Rev.* A **79** 023420
[21] Schmidt M W, *et al* 1993 *J. Comp. Chem.* **14** 1347–1363
[22] Della Picca R, Fainstein P D, Martiarena M L and Dubois A 2008 *Phys. Rev.* A **77**(2) 022702
[23] Paul P M, Toma E S, Breger P, Mullot G, Augé F, Balcou P, Muller H G and Agostini P 2001 *Science* **292** 1689–1692
[24] Kazansky A K, Sazhina I P and Kabachnik N M 2010 *Phys. Rev.* A **82**(3) 033420
[25] Kazansky A K, Grigorieva A V and Kabachnik N M 2012 *Phys. Rev.* A **85**(5) 053409